Study of Conformational as well as Spectral Analysis of 2-[((-1-benzyl-*1H*-1, 2, 3-triazol-4-yl) methyl) thio]-3-Phenylquinazolin-4 (-*3H*)-one through DFT Approach

By

Aniruddh Prasad Chaudhary, Shailendra Kumar Bharti,
Lubna Azmi and Padam Kant

ISSN 2319-3077 Online/Electronic
ISSN 0970-4973 Print

UGC Approved Journal No. 62923
MCI Validated Journal
Index Copernicus International Value
IC Value of Journal 82.43 Poland, Europe (2016)
Journal Impact Factor: 4.275
Global Impact factor of Journal: 0.876
Scientific Journals Impact Factor: 3.285
InfoBase Impact Factor: 3.66

J. Biol. Chem. Research
Volume 34 (2) 2017 Pages No. 787-803

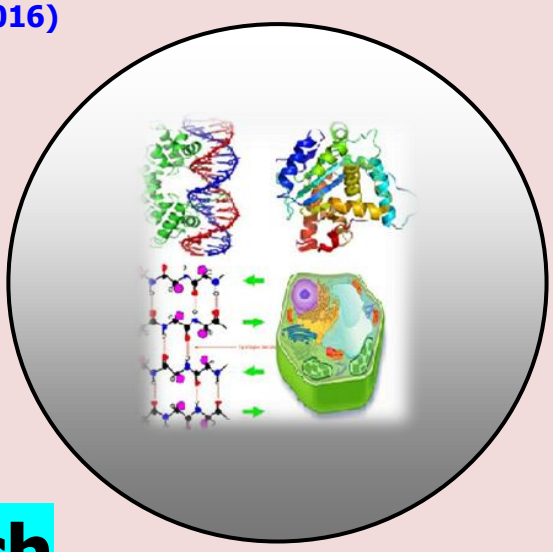

Journal of Biological and Chemical Research

An International Peer Reviewed / Referred Journal of Life Sciences and Chemistry

Indexed, Abstracted and Cited in various International and National Scientific Databases

Published by Society for Advancement of Sciences®

J. Biol. Chem. Research. Vol. 34, No. 2: 787-803, 2017
(An International Peer Reviewed / Refereed Journal of Life Sciences and Chemistry)
Ms 34/02/992/2017

ISSN 2319-3077 (Online/Electronic)
ISSN 0970-4973 (Print)

Aniruddh P. Chaudhary
http:// www.sasjournals.com
http:// www.jbcr.co.in
jbiolchemres@gmail.com

RESEARCH PAPER

Received: 14/11/2017 **Revised: 27/11/2017** **Accepted: 01/12/2017**

Study of Conformational as well as Spectral Analysis of 2-[((-1-benzyl-*1H*-1, 2, 3-triazol-4-yl) methyl) thio]-3-Phenylquinazolin-4 (-*3H*)-one through DFT Approach

Aniruddh Prasad Chaudhary, Shailendra Kumar Bharti,
Lubna Azmi and Padam Kant
Department of Chemistry University of Lucknow, Lucknow Uttar Pradesh-226007, India

ABSTRACT

The 2-(((-1-benzyl-1H-1, 2, 3-triazol-4-yl)methyl) thio)-3-phenylquinazolin-4(-3H)-one was analysed by several modern experimental spectroscopic technique such as IR, ^{1}H NMR, ^{13}C NMR and mass spectrometry as well as computational calculations done by DFT/B3LYP approach using 6-13G (d, p) basis set. The calculated value of global reactivity descriptors predicts the reactivity and stability of the molecule. The MESP and counter maps are also indicate the nucleophilic and electrophilic site inside the molecule. The calculated first hyperpolarizability value describes the non-linear optical property and use of titled compound in photovoltaic solar cells. The conformational analysis showed more stable conformer of the molecule and also studied
Key words: NLO, NBO, UV-Visible, IR, Mesp, conformational and Mulliken population analysis.

INTRODUCTION

Long ago, humans and animals constantly facing serious problem through cancer, tuberculosis and many dangerous diseases. These diseases are caused by different types of bacteria, virus and fungi. In literature survey we found that Quinazolinone and 1,2,3 -triazole both motifs have excellent biological and pharmacological activities.[Mukherjeea et al., 2014, Khan et al., 2014]Quinazolinone derivatives show a large number of biological activities such as, antimicrobial,[Bouley et al., 2016] anti-HIV,[Laddha and Bhatnagar, 2009, Wang et al., 2012] anti-diabetic,[Khan et al., 2016] anticancer,[Al-Obaid et al., 2009, Kamal et al., 2011] anti-inflammatory,[Abdel-Aziz et al., 2016, Alagarsamy et al., 2002, Amin et al., 2010, Manivannan et al., 2011] antagonists activity [Andrews and Cox, 2016, Abou-Seri et al., 2011], anticoagulant activity [Chang et al., 2003], cellular phosphorylation inhibition [Fry et al., 1994] and GABA (Gamma amino butyric acid) receptors in the central nervous system [Lewerenz et al., 2003]. Some drugs have Quinazolinone moiety like proquazone, afloqualoneand diproqualone are used as non-steroidal anti-inflammatory, muscle relaxant and anti-analgesic drugs, respectively.[Kashawa et al., 2009, Reddy et al., 2015] On the other hand 1,2,3-triazoles are ableto form hydrogen bonding, which increases solubility of compound and are also responsible for binding of bimolecular targets [Jadhav et al., 2017].The

compounds containing 1,2,3-triazole based nucleus have a broad spectrum of biological activities such as antifungal [Shaikha et al., 2016], antitubercular [Kumar et al., 2017], antiallergic,[Zhao et al., 2012]antibacterial,[Selvam et al., 2005] anti-HIV [Wang et al., 2016], α-glycosidase inhibitor [Wenqiang et al., 2016, Wang et al., 2016], anticonvulsant, [Suresh et al., 2010] antitumor [Ullaha et al., 2015], antiviral activity [El-Etrawy and Abdel-Rahaman, 2010] and antiplasmodial activity [Devender et al., 2017]. Several marketed drugs such as carboxyamidotriazole, cefatrizine, tazobactam, and rufinamide have 1,2,3- triazole moiety as pharmacophoric unit in the molecule. The titled compound was characterized by recently used spectral technique such as UV-Visible, FT-IR, ^{1}H NMR, ^{13}C NMR and Mass analysis. Its experimental spectral data further correlated theoretically computed spectral data. These theoretical data are calculated by density functional theory using B3LYP functional and 6-31G (d, p) basis set. The curiosity of NLO study of titled compound have been developed because its use as optical modulation, optical switching and photovoltaic solar cells etc. The study of UV-Visible spectrum, HOMO-LUMO gaps energy explained chemical reactivity and stability of molecule. By using Koopmans's theorem we easily calculated global reactivity descriptor's and further proved reactivity and stability of molecule. The MEP surface and counter map indicates electrophilic and nucleophilic centre inside the titled compound.

Experimental Protocol

The titled compounds are synthesized by already known pathway for their computational study through DFT approach [Koohshari et al., 2012]. All synthetic routes of titled compound from its starting materials are summarized below.

Synthesis of 2-mercapto-3-phenylquinazolin-4(3H)-one: A mixture of anthranilic acid (1.0g, 7mmol) ,Phenyl isothiocyanate (1.0ml, 7mmol) and triethyl amine (1.0ml, 7 mmol) in 20 ml absolute ethanol was refluxed for 5 hrs. After completion of the reaction (TLC) mixture was cooled at room temperature and poured into ice cold water with stirring and filtered the precipitate so formed was crystallized from methanol to give crystals of compound (I).

Synthesis of 3-phenyl-2-(prop-2-yn-1-ylthio) quinazolin-4(*3H*)-one

The compound (I) (0.5g, 2.0mmol) taken in round bottom flask and dissolved in DMF (10ml) added Sodium hydride (0.05g, 2mmol) 1.1 equivalent at 0^0C. The mixture stirred about 30 min at 0^0C then propargyl bromide (1.0 ml 2mmol) was added and reaction mixture refluxed for 4-6 hrs. After completion of reaction (TLC) the organic layer separated with ethyl acetate and water. The solvent of organic layer dried over sodium sulphate and evaporated to afford crude compoundwhich is purified by column chromatography usingethyl acetate & hexane as eluent.

Synthesis of synthesized 2-[((-1-benzyl-*1H*-1, 2, 3-triazol-4-yl)methyl) thio]-3-phenylquinazolin-4(-*3H*)-one

3-phenyl-2-(prop-2-yn-1-ylthio) quinazolin-4(*3H*)-one (0.5g, 0.0017mol) and Benzyl azide (0.227g, 1.7mmol) in t-butanol and water(1:1, 20ml) $CuSO_4$-$5H_2O$ (0.272g, 1.7mmol) and Na-ascorbate (0.338g, 1.7mmol) were added and stirred the reaction mixture at room temperature until completion of starting material (approximately 2-3 hrs). The reaction mixture was monitored by TLC. After completion of reaction separate organic compound with ethyl acetate-water and washed with brine and sat. $NaHCO_3$soln, dried over anhyd. Na_2SO_4, evaporated and purified by silica gel column chromatography by using ethyl acetate/ hexane as eluent to give synthesized compound in 78% yield (0.39 g). Molecular Formula $C_{24}H_{19}N_5OS$ IR (KBr in cm^{-1}) 3350, 1680, 1547, 762, 694, ^{1}H-NMR (400MHz, DMSO-d6) δ-(ppm) 8.08 (1H,d, *J* = 8Hz,Ar-H), 7.67(1H,t, *J* = 8Hz,Ar-H), 7.56 (1H,d, *J*= 8Hz,Ar-H),7.49-7.46 (4H,m, *J*=8.0Hz,3xAr-H+ Triazolyl CH), 7.53(2H,d, *J* = 8.0Hz), 7.49 (2H,t,*J*= 8Hz), 7.35-7.21 (3H, m, *J*= 8Hz,Ar-H)5.51(2H,s),4.51 (2H,s), ^{13}C-NMR (100MHz, DMSO-d6) δ-(ppm) 26.86, 52.81, 119.6, 124.18, 126.60, 126.23, 126.13 127.93, 127.56, 127.03, 128.94, 128.76, 128.44, 128.34, 128.16, 129.56, 129.42, 130.00, 131.13, 135.97, 135.75, 147.23, 156.6, 160.8: ESMS: m/z 426.3 $[M + 1]^+$ Calculated m/z 425

RESULT AND DISCUSSION

Computational detail

All the quantum chemical calculations are carried out with Gaussian 09 program package through DFT approach by usingB3LYP functional and 6-31G (d,p) as basis set.

A global minimum for titled compound was obtained by studies of the potential energy curves. ^{1}H&^{13}C NMR chemical shifts, UV–Visible, vibrational wave numbers and NLO properties were computed from optimized geometry of titled compound.

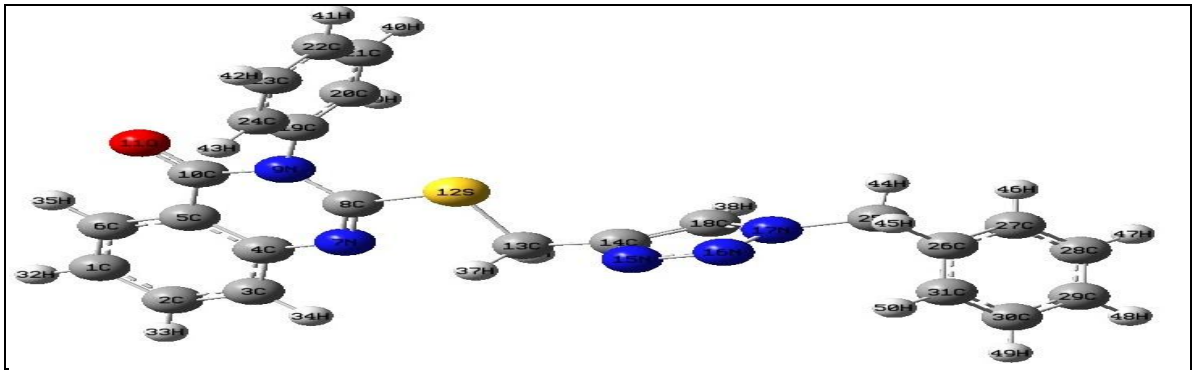

Figure 1 Optimized geometry product.

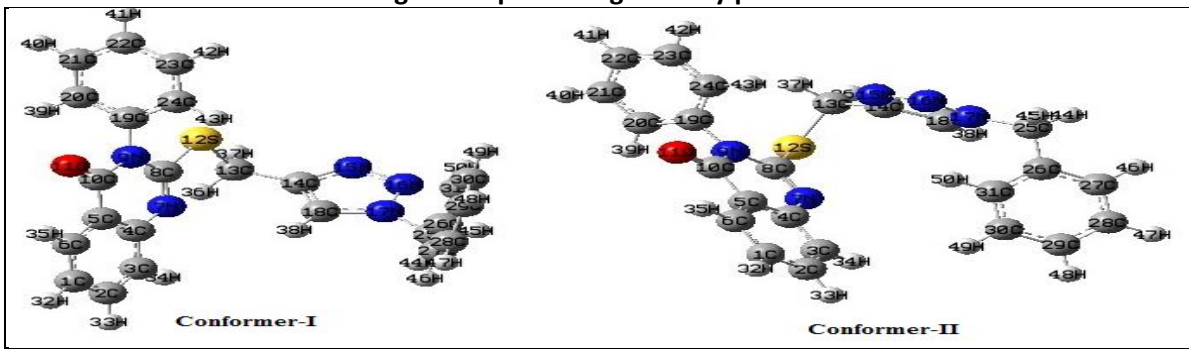

Figure 2. Most stable conformation of titled compound.

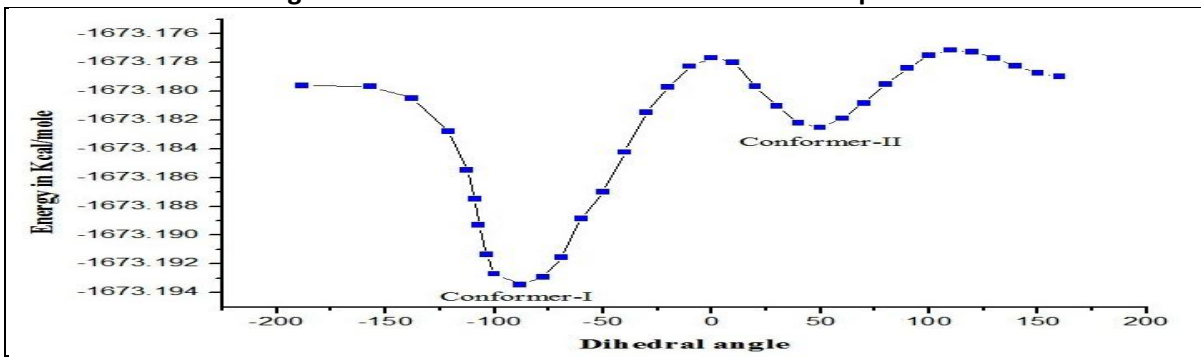

Figure 3. Energy profile (scanning profile) diagram for titled compound.

Conformational analysis

The arrangements of molecule in three dimensional spaces through rotation about σ bonds are called their conformations and this phenomenon is commonly called as conformation isomerism. Conformational analysis is responsible for structure activity relationship. Potential energy surface means relationship between potential energy and molecular geometry which is necessary for all conformation of titled compounds. This potential energy surface scan for titled compound can be calculated with help of DFT/B3LYP functional using 6-13G (d, p) basis set in gas phase.

For the study of more stable conformation of the synthesized compound the scan was performed by s (C8-S12-C13-C14) dihedral angle at step 10^0. In scan dihedral against energy diagram two minima obtained with different energy. The more stable conformer shows minimum energy at -1673.193a.u and less stable conformer shows maximum energy -1673.182a.u are depicted in Figure [3]. The energy difference between conformer I and conformer II are 0.011 Kcal/mole. This energy difference indicates that both conformations are stable but conformer I is more stable than second conformer II The structure of both conformer are shown in Figure [2].

UV-Visible Spectroscopy, HOMO-LUMO and Global reactivity descriptors

In order to understand nature of several electronic transition of synthesized compound observed in UV-Visible spectrum at singlet-singlet level was calculated by completely optimized geometry using TD-DFT/B3LYP methods and 6-13G (d, p) basis set. The correlation between experimental (DMSO) and theoretical calculated excitation energies, oscillator strength(f) and their assignment with contribution in gas as well as solvent phase are summarized in Table.[1] The correlation graph of observed and computed UV-Visible spectra in gas as well as solvent phase are plotted among intensity (ε = L mol-1 cm-1) against wavelength (λ_{nm}) reported in Figure.[4] The experimentally observed wavelengths of absorption maximum (λ_{max}) values in DMSO are 278 and 314 nm respectively. However theoretically observed absorption maximum in gas as well as in DMSO are 217.40, 216.32 and 285.33, 290.75 nm they can be assigned to π → π* transitions in titled compound, respectively. Thus we can conclude that these values have good correlation with computed value.

Table 1. Calculated and experimental electronic excitations for (3): *E* / eV, oscillatory strength (*f*), (λ_{max} / nm) at TD–DFT/B3LYP/6–31G (d,p) level.

Excitations	Solvents	λ_{max} Exp.	λ_{max} calcd.	E (eV)	(*f*)	Contributions %	Assignment
111→112	Gas	314	334.63	3.7051	0.1006	44%	$\pi \rightarrow \pi^*$
(H→L)	DMSO		335.91	3.6910	0.1366	46%	
110→113	Gas	278	284.36	4.2059	0.1245	22%	$\pi \rightarrow \pi^*$
(H-1→L+1)	DMSO		286.25	4.2059	0.1352	18%	

Table 2. HOMO, LUMO global electronegativity, hardness and softness, electrophilicity index.

Parameter	2-(((-1-benzyl-1H-1, 2, 3-triazol-4-yl)methyl) thio)-3-phenylquinazolin-4(-3H)-one	
	Gas phase	Solvent (DMSO)
ε_H (eV)	-0.21217	-0.21917
ε_L (eV)	-0.05500	-0.06123
ε_L–ε_H gap (eV)	0.15717	0.15794
Chemical hardness(η)(eV)	0.07858	0.07897
Global softness(σ)(eV)	6.3625	6.3315
Electronegativity(χ)(eV)	-0.07858	-0.07897
Electrophilicity index(ω)(eV)	0.1135	0.1244
Chemical potential(μ)	-0.1336	-0.1402

The HOMO -LUMO are Frontier molecular orbitals (FMO) and the energy of these orbitals is helpful for measuring electron donor and electron acceptor molecular orbitals, respectively. With the help of FMO we can predicts many types reactions which involves excitation of electron from HOMO to LUMO.

The larger value of energy of HOMO represents good electron donor tendency of molecular orbital however lower value of LUMO represents weak electron acceptor tendency of molecular orbital. The HOMO-LUMO energy gap play significant role in electron transport, chemical reactivity, optical polarizability and kinetic stability of molecule. The excitation of H→ L and H−1 → L+1 are labelled in Figure [5]. The energy gaps as well as percentage contribution of H→ L and H−1 → L+1 transitions are 3.6910 (ev), 46% and 4.2059(ev), 18% respectively. The lower value of HOMO to LUMO showed easier molecular charge transfer inside the titled compound.

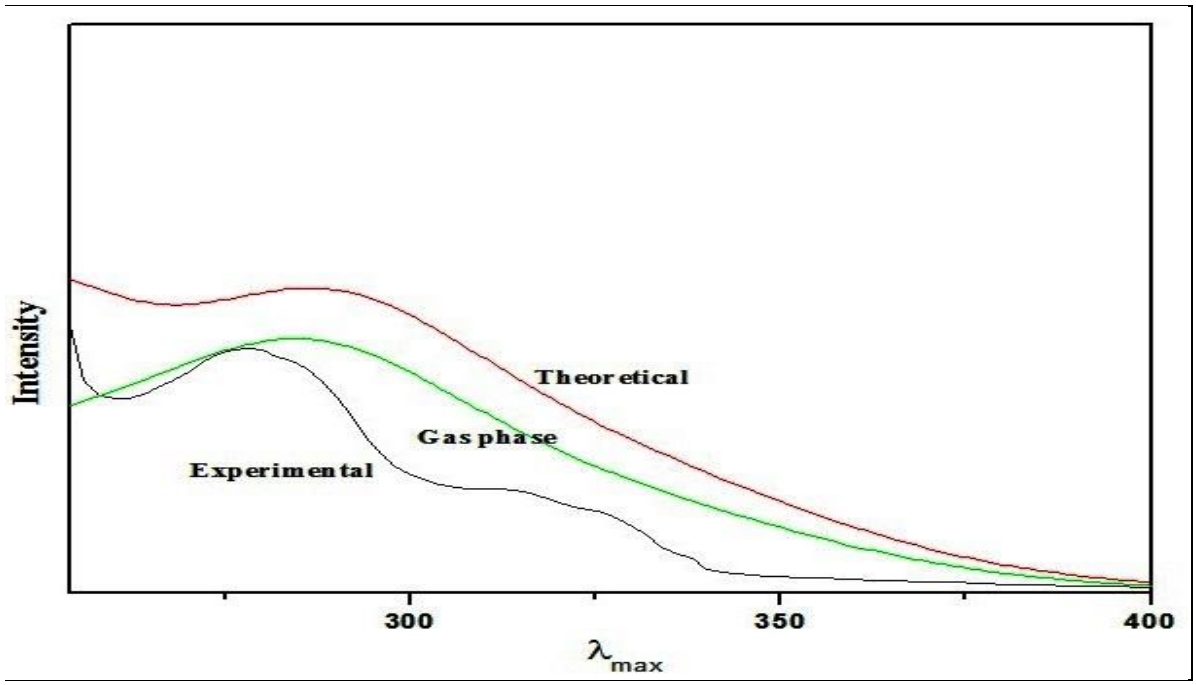

Figure 4. Comparison between Experimental and theoretical UV-Visible spectrum.

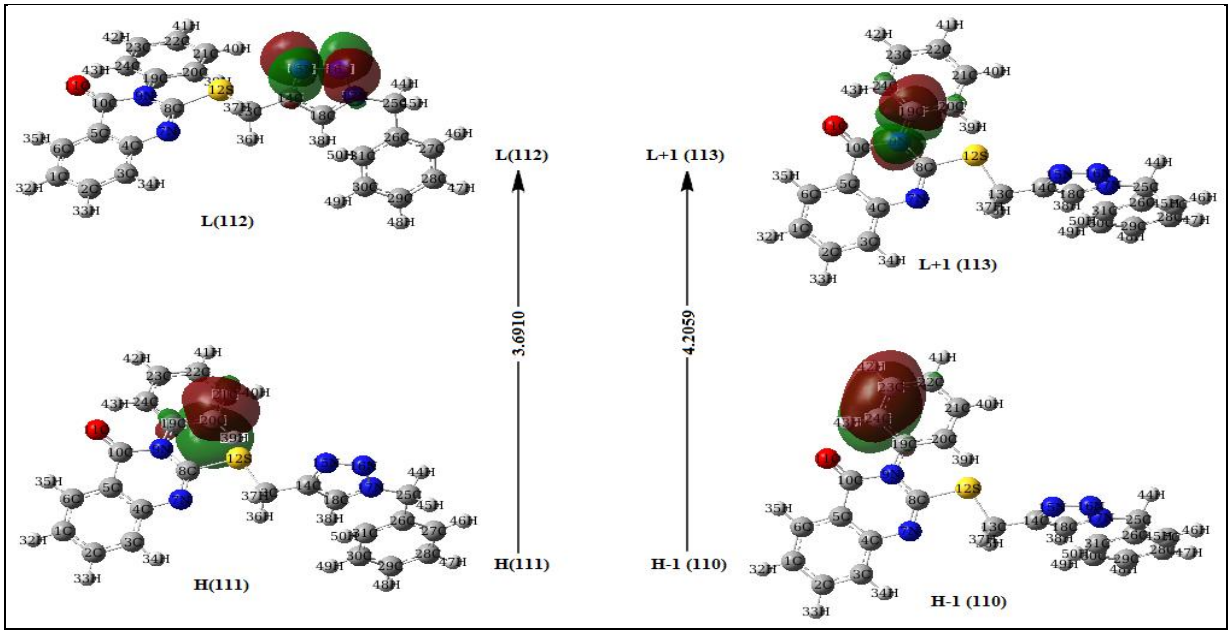

Figure 5. HOMO-LUMO of UV-Visible spectrum.

By using Koopmans's theorem as well as HOMO and LUMO energy of frontier molecular orbitals calculated electro negativity (χ)= $-1/2(\varepsilon_{LUMO} + \varepsilon_{HOMO})$, chemical potential ($\mu$) = 1/2 ($\varepsilon_{LUMO} + \varepsilon_{HOMO}$), chemical hardness ($\eta$) = 1/2 ($\varepsilon_{LUMO} - \varepsilon_{HOMO}$), global softness ($S$) = $1/2\eta$ and electrophilicity index (ω) = $\mu^2/2\eta$. The all value of global reactivity descriptors calculated gas as well in DMSO solvent are listed in Table [2]. The electrophilic index and negative value of chemical potential are measure stability of molecule. Global softness and chemical hardness are related to the polarisable property of molecule. Highest polarisablemolecule has large softness value and lower polarisable molecule has less polarisable tendency.

Vibrational Assignment

The theoretical vibrational wave number computed for newly synthesized 2-[((-1-benzyl-*1H*-1, 2, 3-triazol-4-yl)methyl) thio]-3-phenylquinazolin-4(-*3H*)-one with the help of Gaussian 09 program and their potential energy distribution analysis made by Gar2ped software. The correlations between experimental and theoretical wave numbers are shown in Table [3]. The values of theoretical wave numbers are larger in comparison with experimental values for several normal modes of vibrations. This dissimilarity arises due to following two reasons. The first reason is environment that means the theoretical value calculated in gas phase however experimental value observed in solid phase and the second reason is anharmonicity and harmonicity that means the experimental is anharmonic while theoretical is harmonic wave number. Therefore, the theoretical values are scaled down by factor 0.9608 for removal of anharmonicity present in real system. The computed and experimental FT-IR spectrum of titled compound is expressed in Figure [6].

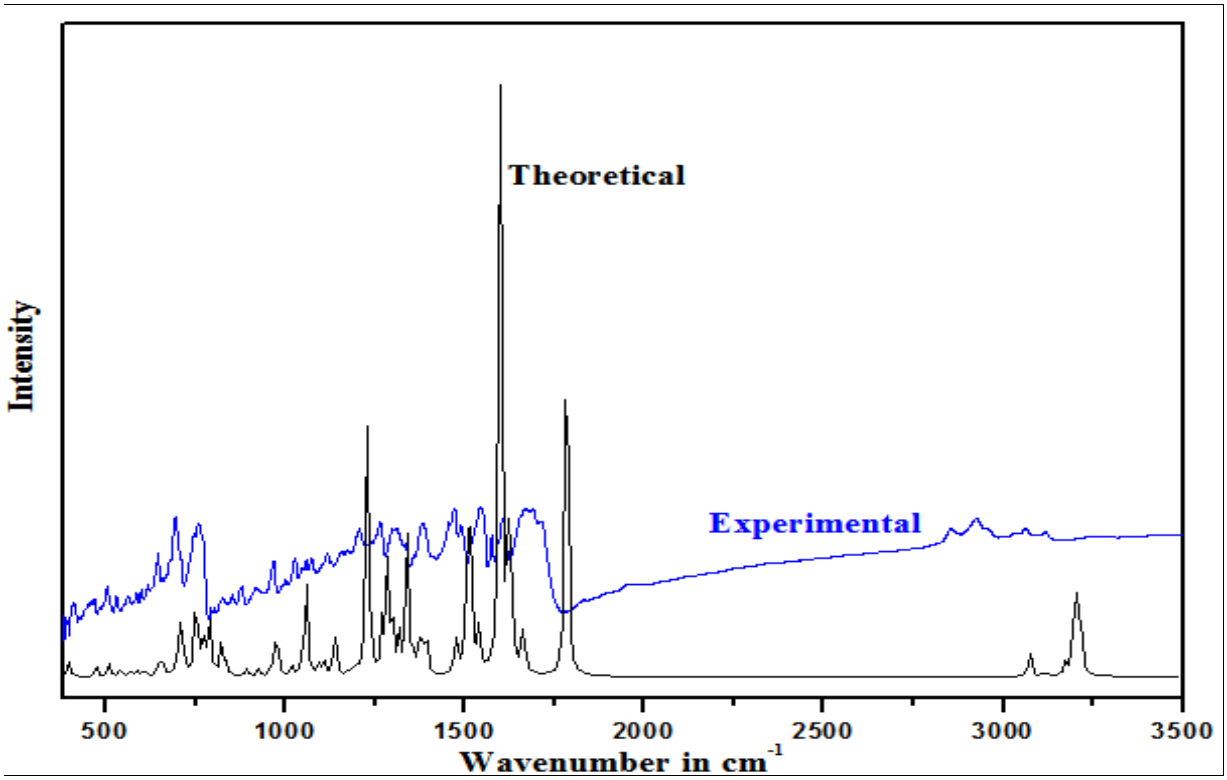

Figure 6. Comparison between theoretical and experimental IR spectra for titled compound.

C=O Vibration: The strong C=O (vC10O11) stretching FT-IR band observed at 1680 cm^{-1} and theoretical value at 1714 cm^{-1}. The experimental value is less than normal carbonyl groups because C=O groups attached to the highly electronegative atoms which shows conjugation through inductive effect.

Table 3. Experimental and calculated (selected) vibrational wave numbers of monomer using B3LYP/6-31G(d,p) and their assignments [harmonic wave numbers (cm-1), IR int(Kmmol-1)].

Wave number unscaled	Wave number scaled	Exp. Wave numbers	Exp.IR_{int}	Assignment(PED) ≥ 5 %
3294	3165	3118	15.13	ν(C18H38)(78.)
3221	3095		5.69	ν(C23H43)(68.)ν(C24H42)(18.)-ν(C21H40)(10.)
3215	3089	3072	8.9	ν(C3H34)(78.)ν(C2H33)(11.)-ν(C6H35)(10.)
3210	3084		17.65	ν(C29H48)(41.)ν(C30H49)(28.)ν(C28H47)(22.)ν(C31H50)(6.)
3205	3079	2931	24.49	ν(C22H41)(40.)-ν(C24H43)(21.)-ν(C20H39)(20.)ν(C23H42)(12.)ν(C21H40)(6.)
3202	3077		15.2	ν(C1H32)(61.)ν(C2H33)(17.)-ν(C6H35)(12.) -ν(C3H34)(9.)
3200	3074	2838	22.87	ν(C28H47)(38.)-ν(C30H49)(33.)-ν(C31H50)(22.)
3172	3048		8.05	ν(C27H46)(81.)-ν(C28H47)(14.)
3074	2954		19.44	ν(C25H44)(64.)ν(C25H45)(35.)
1784	1714	1680	337.83	(δas-R2)(57.) (δas-R5)(20.) -δ(C8S12C13)(5.)-δ(N7C8S12)(5.)
1663	1598		11.4	(δas-R2)(10.) δ(C8S12C13)(9.) δ(N7C8S12)(8.) (δas-R5)(8.)-ν(C30C31)(8.)-ν(C27C28)(8.) -(δas-R2)(7.)LINν(C1C2)(C8N7)(6.)
1663	1598		30.82	δ(C8S12C13)(16.) δ(N7C8S12)(16.) (δas-R2)(14.) (δas-R5)(12.) -(δas-R2)(9.)LINν(C1C2)(C8N7)(8.)
1624	1560	1605	163.06	δ(N7C8S12)(33.) δ(C8S12C13)(23.) -LINν(C1C2)(C8N7)(18.) -(δas-R2)(13.) -ν(N7C8)(7.)
1599	1536	1547	580.74	δ(N7C8S12)(40.) ν(C14N15)(9.)ν(C8S12)(5.)
1541	1481		9.56	δ(C29C30H49)(16.) -δ(C27C28H47)(15.)δ(C30C31H50)(13.) -δ(C26C27H46)(12.)-ν(C29C30)(10.)ν(C26C31)(8.)-ν(C28C29)(8.)ν(C26C27)(7.)
1537	1477	1469	31.32	δ(N7C8S12)(31.)-δ(C20C21H40)(9.) δ(C22C23H42)(9.) δ(C23C24H43)(7.)-δ(C19C20H39)(7.) δ(C8S12C13)(6.)ν(C19C20)(5.)ν(C19C24)(5.)-ν(C22C23)(5.)-ν(C21C22)(5.)
1513	1454	1459	150.86	δ(N7C8S12)(23.) -(δas-R2)(20.) -ν(C4N7)(14.)ν(C4C5)(13.)LINν(C1C2)(C8N7)(7.)
1507	1448	1392	36.95	LINν(C1C2)(C14C18)(35.) -δ(C14C18H38)(16.)-ν(N17C18)(9.) -δsc(C25H44H45)(7.)-δsc(C13H36H37)(7.) -(δas-R4)(5.)
1393	1338	1373	32.53	(ρ– CH2)(26.) -(ω–C18H38)(21.)LINν(C1C2)(C18N17)(16.) δsc(C13H36H37)(6.)
1385	1330		8.34	δ(C8S12C13)(29.)-δsc(C13H36H37)(20.)-δsc(C13H36H37)(19.)(δas-R4)(5.)LINν(C1C2)(C18N17)(5.)
1376	1322	1313	37.59	δ(N7C8S12)(40.) -(δas-R2)(33.)ν(C4C5)(8.) -LINν(C1C2)(C8N7)(6.)
1339	1287	1263	93.58	δ(N7C8S12)(52.)LINν(C1C2)(C8N7)(36.)
1337	1285		10.42	δ(N7C8S12)(48.)LINν(C1C2)(C8N7)(31.)
1316	1264		26.2	δ(C8S12C13)(31.)ν(C8S12)(21.) (δas-R5)(17.) (δas-R2)(9.) -(δas-R2)(6.)
1299	1248		30.1	ν(N15N16)(31.) -(δas-R4)(23.)(δas-R4)(17.) -δ(C14C18H38)(9.) -LINν(C1C2)(C14C18)(5.)
1286	1235	1206	89.74	δ(N7C8S12)(38.) δ(C8S12C13)(25.) -(δas-R2)(9.)LINν(C1C2)(C8N7)(7.)
1270	1220		45.16	LINν(C1C2)(C14C18)(43.)-δ(C8S12C13)(35.) ν
				(C12C13)(8.)(ω–C18H38)(6.)

Table 3 Continued

1229	1181	1113	183.17	ν(C8S12)(33.) δ(C8S12C13)(27.) -LINν(C1C2)(C8N7)(18.) (δas-R2)(7.)-ν(C8N9)(5.)
1135	1091	1066	15.16	δ(N7C8S12)(38.) (δas-R5)(18.) -LINν(C1C2)(C8N7)(12.) -(δas-R2)(8.)
1059	1018	1040	55.58	LINν(C1C2)(C18N17)(23.)(δas-R4)(22.)δ(C14C18H38)(13.) -LINν(C1C2)(C18N17)(12.)(ω–C18H38)(9.)(δas-R4)(7.)
976	937	967	39.19	ν(C8S12)(29.)-δ(N7C8S12)(28.) δ(C8S12C13)(21.) -LINν(C1C2)(C8N7)(16.)
837	804	880	8.45	δ(C8S12C13)(54.)ν(C8S12)(37.)
822	789	769	25.68	(ω–C18H38)(53.) -LINν(C1C2)(C18N17)(35.)LINν(C1C2)(C14C18)(6.)
786	755	762	43.81	(R2-Puckering)(38.) -δoop(C8S12)(22.) -(ω–C18H38)(10.)LINν(C1C2)(C18N17)(9.)
772	742		21.25	LINν(C1C2)(C18N17)(44.) -(ω–C18H38)(43.)-δsc(C13H36H37)(5.)
751	722	738	69.25	LINν(C1C2)(C18N17)(40.) -(ω–C18H38)(29.)LINν(C1C2)(C14C18)(16.)-δsc(C13H36H37)(8.)
705	678	694	28.8	LINν(C1C2)(C8N7)(26.)-δ(C8S12C13)(15.) -(R3-Puckering)(11.)LINν(C1C2)(C14C18)(7.)LINν(C1C2)(C18N17)(7.) -(δas-R5)(6.)
705	677		14.94	(τ– R2)(22.) -δoop(C8S12)(17.) δoop(N9C19)(14.) -(R1-Puckering)(9.) -LINν(C1C2)(C8N7)(9.) -δoop(C10O11)(6.) (R2-Puckering)(5.)
648	623		13.71	δsc(C13H36H37)(22.) δ(N7C8S12)(21.)LINν(C1C2)(C8N7)(19.)-ν(C12C13)(12.)LINν(C1C2)(C14C18)(8.)(ω–C18H38)(7.)LINν(C1C2)(C18N17)(5.)

Proposed assignment and potential energy distribution (PED) for vibrational modes: Types of vibrations: ν– stretching, δsc – scissoring, ρ – rocking, ω – wagging, δ-deformation, δs – symmetric deformation, δas – asymmetric deformation, τ – torsion.

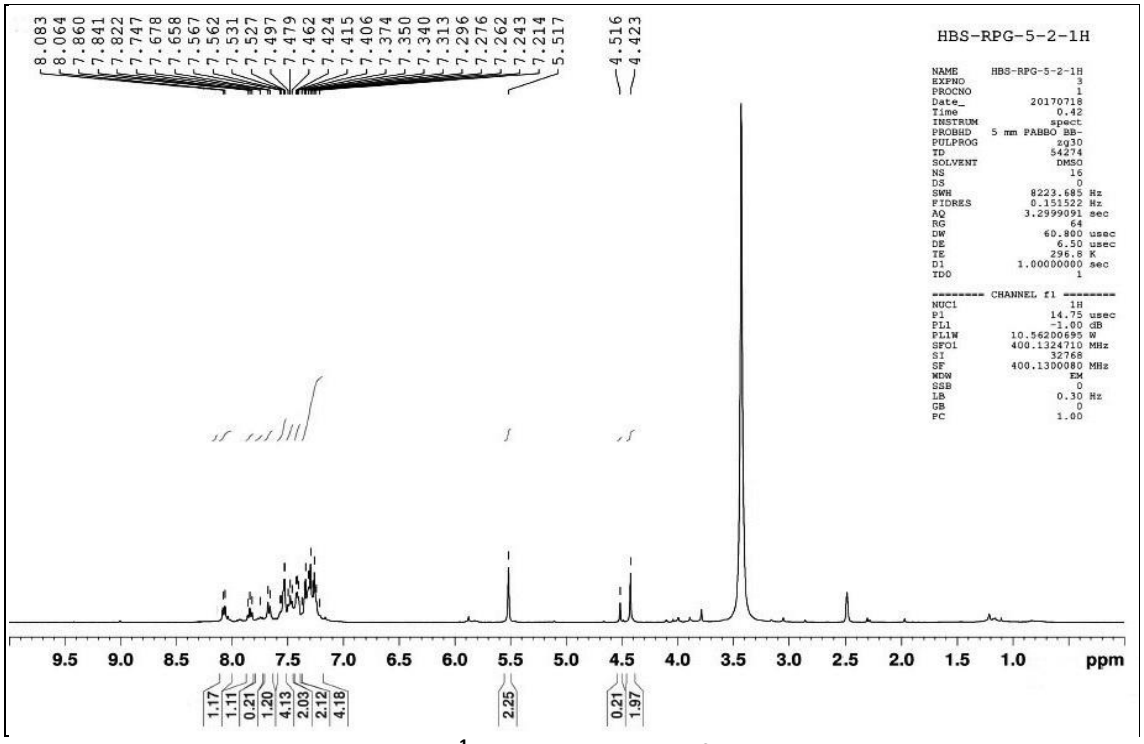

Figure 7. Experimental ^{1}H NMR spectrum of in DMSO-d6 solvent.

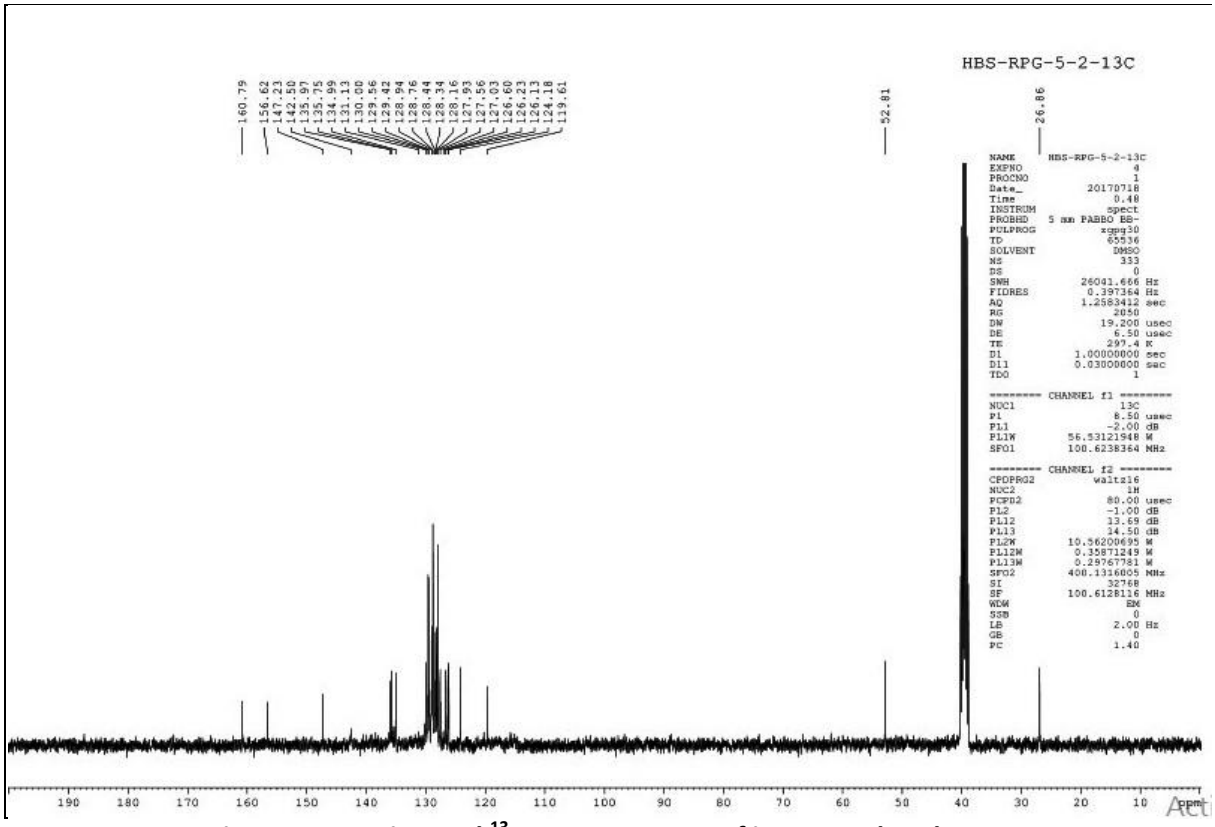

Figure 8. Experimental ^{13}C NMR spectrum of in DMSO-d6 solvent.

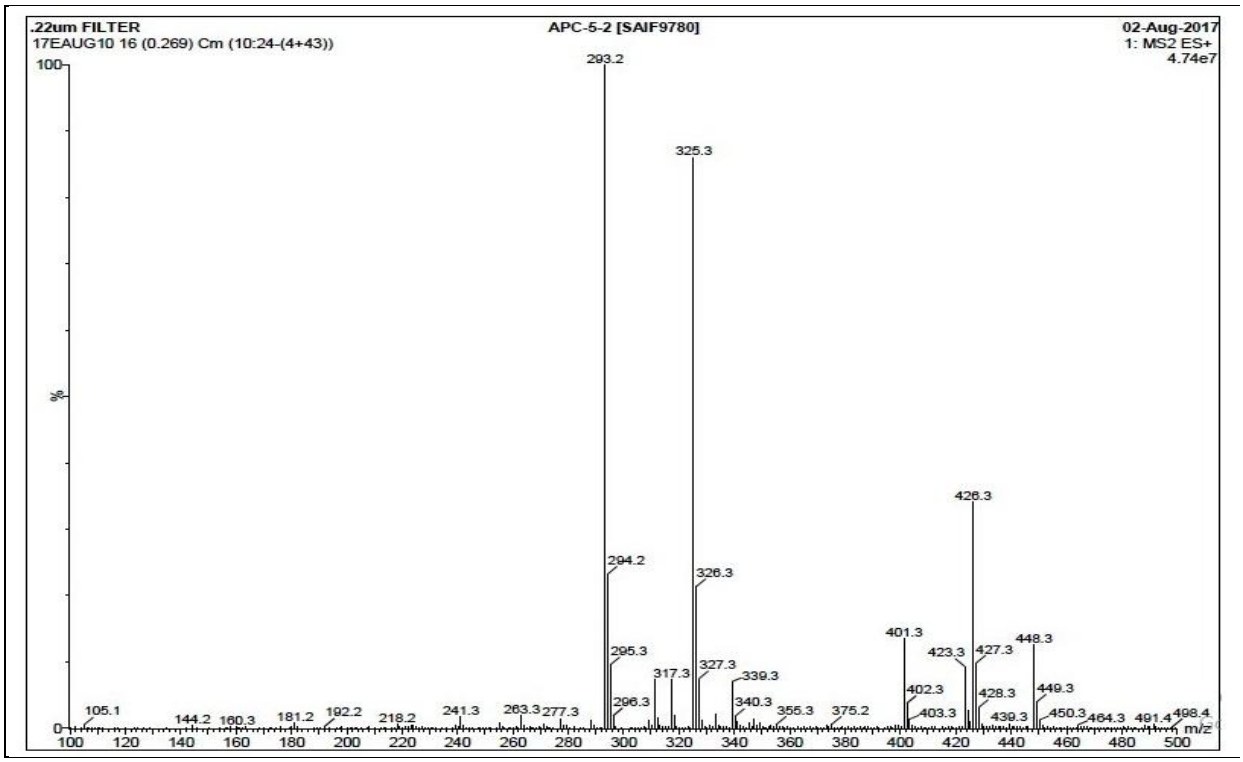

Figure 9. Experimental mass spectrum.

The normal C=O stretching frequency reported at 1720-1680 cm^{-1}[32].

C-C Vibration: For the C-C stretching vibration the reported value at 1312 and 1571cm^{-1} [33]. In present synthesized compound the experimental C-C stretching vibration observed at 1313 and 1459 cm^{-1} however the theoretical computed value at 1322 and 1454 cm^{-1}.

C=N and C-N Vibration: The C=N stretching vibration of benzaoxinone moiety reported at 1582cm^{-1}. [34] For synthesized compound the C=N stretching vibration observed at 1547 cm^{-1} and theoretical calculation observed at 1536 cm^{-1}. The correct analysis of C-N vibration is very tough because mixing of many bands in this region. Since the C-N vibration clearly identified by animation application of Gauss view 5.0 programs. In triazole moiety the C-N stretching vibration is reported at 1339 cm^{-1}. [34]

On the basis of this value we observed C-N stretching at 1373 cm^{-1} experimentally however theoretical calculation gives at 1338 cm^{-1}.

=C-H and C-H Vibration: For =C-H (triazole) the FT-IR stretching value reported at 3043 cm^{-1}. [35] In titled compound =C-H (triazole) stretching frequency experimentally observed at 3118 cm^{-1} however theoretically observed at 3165 cm^{-1}. The experimental and theoretical value is greater than reported value due to the =C-H bond attached to the nitrogen atoms which increases the force constant between C=C-H bond. In literature study we found that the aromatic C-H stretching mode reported at 3095 cm^{-1}[36]. The C-H stretching vibration observed in FT-IR spectrum at 2931 and 3072 cm^{-1} while theoretical computation gives at 3079 and 3089 cm^{-1}. Both experimental and calculated values have good agreement which confirm the synthesized compound.

^{1}H NMR and ^{13}C NMR spectroscopy

The correlations between experimental and theoretical 1H NMR as well as 13C NMR chemical shift values are labelled in Table [4] and Table [5]. The chemical shift valuesin solvent phases as well as gas phase were calculated by GIAO approach using DFT/B3LYP method and 6-13G (d, p) basis set. The experimental chemical shifts of 2-[((-1-benzyl-*1H*-1, 2, 3-triazol-4-yl)methyl) thio]-3-phenylquinazolin-4(-*3H*)-one has good agreement with theoretical value. The residual value of ^{1}H NMR and^{13}C NMR are obtained by subtractions of experimental values from theoretical values observe in gas phase. For ^{1}H NMR as well as ^{13}C NMR root mean square deviation (RMSD) reported are 0.11 and 2.1 respectively. The experimental 1H NMR and 13C NMR spectra are shown in Figure [7] & [8] respectively.The aromatic protons have higher chemical shift values due to anisotropic effects it shows diamagnetic deshielding. The Triazolyl proton (H38) appears at 7.49-7.46 ppm shows formation of 1,2,3- triazole ring inside the synthesize compounds.

The appearance of two different peak in proton NMR spectroscopy at 4.51ppm (H36, H37) and 5.51ppm (H44, H45) which indicates triazole ring present between two CH_2 groups. The carbonyl carbon appears at 160.8 ppm which represents ($CONH_2$) linkage. In spite of ^{1}H NMR and ^{13}C NMR also seen mass spectrum of titled compounds which confirm the molecular ion peak [M+1] and molecular formula $C_{24}H_{19}N_5OS$. The mass spectrum of titled compound is depicted in Figure [9].

Polarizability and First hyperpolarizability

The computational methods are conventional way for discovery of new compounds which show non-linear optical property. With the help of this method we can easily predicts dipole moment (μ), polarizability (α_0) and first hyperpolarizability (β_0) of new compounds. [Rawat and Singh, 2015, Rawat et al., 2014] These parameters are calculated DFT/B3LYP functional using 6-31G (d, p) basis set.

Table 4. Calculated and experimental ^1H NMR chemical shifts (δ / ppm) of compound in DMSO-d6 solvent at 25 °C.

Atom	Gas phase	DMSO-d6	δexp	Assignment	Residual	Squared Residual	RMSD
H32	7.3576	7.6103	7.49	1H,m of Benzaoxinone ring	-0.13	0.0169	
H33	7.6605	7.95	7.67	1H, t of Benzaoxinone ring	0.02	0.0004	
H34	7.502	7.6474	7.56	1H,d of Benzaoxinone ring	0.06	0.0036	0.11
H35	8.4017	8.3715	8.08	1H,d of Benzaoxinone ring	-0.32	0.1024	
H36	4.2376	4.4249	4.51	2H,s adjacent to the sulfur atom	-0.28	0.0784	
H37	4.4	4.3199					
H38	7.3097	7.7616	7.46	3H, m 2x Ar-H +Triazolyl CH	-0.16	0.0256	
H39	7.3668	7.5328	7.53	2H,d Ar-H	-0.17	0.0289	
H40	7.5213	7.7682	7.47		0.05	0.0025	
H41	7.5243	7.7756	7.31	3H, m Ar-H	0.21	0.0441	
H42	7.5443	7.7489					
H43	7.4205	7.5287	7.53				
H44	4.5843	4.9568	5.51	2H,s of benzylic proton			
H45	5.7872	5.7702			0.27	0.0729	
H46	7.2599	7.5354	7.29	All Proton are appear in aromatic region	0.28	0.0784	
H47	7.398	7.5652	7.46		-0.07	0.0049	
H48	7.392	7.527	7.27		0.12	0.0144	
H49	7.4242	7.5151					
H50	7.4412	7.3717	7.31				

The dipole moment (μ), isotropic polarizability (α_0) and first hyperpolarizability (β_0) are expressed in following equation respectively [42]

$$\mu = \sqrt{\mu_x^2 + \mu_y^2 + \mu_z^2}$$

$$\alpha_0 = \frac{\alpha_{xx} + \alpha_{yy} + \alpha_{zz}}{3}$$

$$\beta_0 = \sqrt{\beta_x^2 + \beta_y^2 + \beta_z^2}$$

Table 5. Calculated and experimental ^{13}C NMR chemical shifts (δ / ppm) of compound in DMSO-d6 solvent at 25 °C.

Atom	Gas phase	DMSO-d6	δexp	Assignment	Residual	Squared Residual	RMSD
C 1	121.98	122.1	123.16	Benzaoxinone carbon	-1.18	1.3924	2.1
C 2	133.55	131.11	134.99		-1.44	2.0736	
C 3	122.09	122.25	124.18		-2.09	4.3681	
C 4	145.35	143.29	147.23		-1.88	3.5344	
C 5	118.59	118.02	119.61		-1.02	1.0404	
C 6	124.89	124.21	126.13		-1.24	1.5376	
C 8	154.23	155.36	156.62	Carbon present between both nitrogen in Benzaoxinone ring	-2.39	5.7121	
C 10	158.43	159.62	160.79	C=O groups due to amide linkage	-2.36	5.5696	
C 13	49.97	51.61	52.81	Methylene carbon adjacent to sulfur atom	-2.84	8.0656	
C 14	138.02	137.61	135.97	Triazolyl carbon	2.05	4.2025	
C 18	129.50	130.50	131.13		-1.63	2.6569	
C 19	139.63	138.86	142.50		-2.87	8.2369	
C 20	125.9	125.5	127.93		-2.03	4.1209	
C 21	124.19	125.24		Benzene ring carbon attached to the Benzaoxinone ring			
C 22	124.58	125.91					
C 23	126.54	127.23	128.34		-1.8	3.24	
C 24	127.22	128.48	129.42		-2.2	4.84	
C 25	68.665	69.56	71.46	Benzylic carbon	-2.79	7.7841	
C 26	133.25	134.54	135.75		-2.5	6.25	
C 27	122.85	124.21		Benzene ring carbon attached to the benzylic carbon			
C 28	123.23	123.74					
C 29	123.56	123.70					
C 30	124.61	124.22	126.60		-1.99	3.9601	
C 31	123.80	123.26			-1.18	1.3924	

Residual = Theoretical values obtained in gas phase minus the experimental values
RMSD = Root mean square deviation

The value of β_0 is the parameter of measurement of NLO property of compounds. The computed first hyperpolarizability is 11.2003×10^{-30}esu reported in Tables [7]. The first hyperpolarizability of titled compound is thirty times greater than that of urea (β of urea 0.3728×10^{-30}esu 6-31G (d, p) respectively. In literature study we find that the compound showing NLO properties are used in various areas like telecommunications, optical modulation, optical switching, signal processing and several optical materials [Anitha et al., 2015, Kishor and Nagaiyan, 2017, Natorajan et al., 2008]. The NLO properties of organic compounds are measured by also HOMO-LUMO energy gap. Lowest the energy gap shows molecule has good NLO activity.

MEP Surface

The MEP surface V(r) calculated with the help of following mathematical equation at given point r(x,y,z) in the adjacent of a molecule

$$V(r) = \sum Z_A/|R_A - r| - \int \rho(r')/|r' - r|\, d^3r'$$

Where Z_A is the charge of nucleus A located at R_A. $\rho(r')$ is the electronic density functions of the molecule, and r' is the dummy integration variable. It is commonly called as electrostatic potential energy maps or molecular electrical potential surfaces. Itis related with dipole moments, electronegativity and chemical reactivity of the molecular systems. It is helpful for illustrating the charge distributions of molecules three dimensionally.

Table 7. Calculated Dipole moment (μ_0), Polarizability ($|\alpha_0|$), anisotropy of Polarizability ($\Delta\alpha$), First Hyperpolarizability (β_0) and their components, using B3LYP/6–31G(d,p).

Dipole moment		Polarizability		Hyperpolarizability	
μx	4.9213	αxx	426.801	βxxx	-571.47
μy	-2.2257	αyy	35.301	βxxy	-541.21
μz	-4.3773	αzz	349.388	βxyy	-182.11
μ	6.9522	αxy	11.216	βyyy	-417.48
		αxz	4.265	βxxz	-271.31
		αyz	206.601	βxyz	13.038
		α0	40.0876	βyyz	17.469
		Δα	121.798	βxzz	184.602
				βyzz	-128.04
				βzzz	-165.7
				β0	11.2003

μ_0 in Debye;$|\alpha_0|$ and $\Delta\alpha$ in 10^{-24} esu; β_0 in 10^{-30} esu,

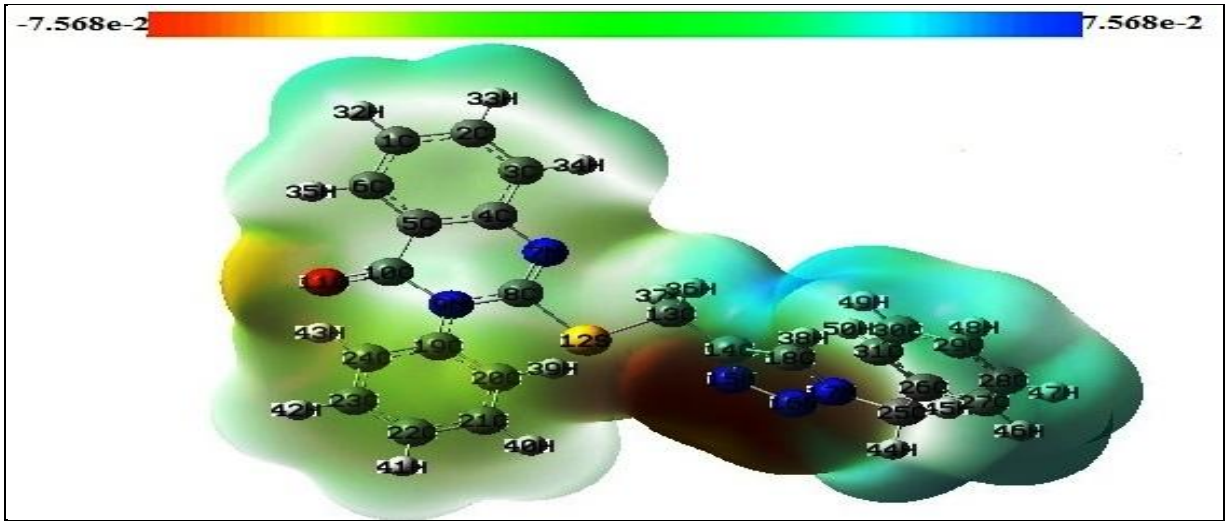

Figure 10. Molecular electrostatic potential (ESP) maps of titled compound.

In MEP analysis, we can predict how molecules interact with one another and charge regions of molecule. The MEP surface and counter map diagramsare shown in Figure [10] and [11] respectively. The blue region specifies low electron concentration and maximum repulsion (highest electrostatic potential), green region shows neutral electrostatic potential region and the red region specifies high electron concentration and maximum attraction (lowest electrostatic potential).

In this way we can conclude that the positive regions (blue & light blue region) have nucleophilic reactivity and negative regions (red & yellow region) have electrophilic reactivity. The MEP map is responsible for determining the hydrogen bonding interaction area of the molecule. The MEP map indicates that the largest negative electrostatic potential value presented around C10 & O11 (-7.568e-2 a.u) however the most positive value found around N9 & N12 (7.568e-2 a.u). So, it is predicted that the most preferred region for electrophilic and nucleophilic attack is around C10 & O11 and N9 & N12, respectively.

CONCLUSION

In present work, the recently synthesized compound is optimized by DFT/B3LYP approach using 6-13G (d, p) basis set. The ^{1}H NMR ^{13}C NMR finds out by GIAO method and calculated RMSD (root mean square density) is 0.11 & 2.1 respectively. Its theoretical Spectral (FT-IR, UV-Visible, NMR and Mass) value well correlated with experimental value. I hoped the titled compound may be used as drug in various clinical purposes on the basis of literature study.

ACKNOWLEDGEMENTS

Aniruddh Prasad Chaudhary is thankful to senior research fellowship (SRF) provided by university grant commission new Delhi India. We also thanks to CDRI SAIF which gives mass spectral analysis facility. And further thanks University of Lucknow because which provides FT-IR, UV, NMR analysis as well as computational facility.

REFERENCES

Mukherjeea D., Mukhopadhyay A, Bhat K. S., Shridharad A. M.,Rao K. S synthesis, characterization and anticonvulsant activity of substituted 4-chloro-2-(4-piperazin-1-yl) quinazolines*Int J Pharm PharmSci*, 6, 567-571, 2014.

KhanI., Ibrar A., Abbas N., Saeed A. Recent advances in the structural library of functionalized quinazoline and quinazolinone scaffolds: Synthetic approaches and multifarious applications*European Journal of Medicinal Chemistry* 76 193-244, 2014.

Bouley R., Ding D.,Peng Z., Bastian M., Lastochkin E, Song W.,Suckow M. A., Schroeder V. A., Wolter W. R.,Mobashery S., Chang M. Structure−Activity Relationship for the 4(3H)‑Quinazolinone Antibacterials*J. Med. Chem*. 59, 5011−5021, 2016.

Laddha S. S., Bhatnagar S. P.A new therapeutic approach in Parkinson's disease: Some novel quinazoline derivatives as dual selective phosphodiesterase 1 inhibitors and anti-inflammatory agents *Bioorganic & Medicinal Chemistry* 17, 6796–6802, 2009.

Wang Z., Wang M., Yao X., Li Y., Tan J., Wang L., Qiao W., Geng Y., Liu Y., Wang Q. Design, synthesis and antiviral activity of novel quinazolinones *European Journal of Medicinal Chemistry* 53, 275-282, 2012.

Khan I., Zaib S., Batool S., Abbas N., Ashraf Z., Saeed A. Quinazolines and quinazolinones as ubiquitous structural fragments in medicinal chemistry: An update on the development of synthetic methods and pharmacological diversification*Journal of Bioorganic & Medicinal Chemistry*24, 2361-2381, 2016.

Al-ObaidA.M., Abdel-Hamide S. G.,El-Kashef H. A, Abdel-Aziz A.A.-M., Azab Hamad A. S. E., Khamees A. A., El-Subbagh H. I., Substituted quinazolines, part 3. Synthesis, in vitro antitumor activity andmolecularmodeling study of certain 2-thieno-4(3H)-quinazolinone analogs*European Journal of Medicinal Chemistry* 44, 2379–2391, 2009.

Kamal A., Bharathi E. V., Reddy J. S., Ramaiah M. J., Dastagiri D., Reddy M. K., Viswanath A., Reddy T. L., Shaik T. B.,. Pushpavalli S.N.C.V.L, Bhadra M. P. Synthesis and biological evaluation of 3,5-diaryl isoxazoline/isoxazole linked 2,3-dihydroquinazolinone hybrids as anticancer agents *European Journal of Medicinal Chemistry* 46, 691-703, 2011.

Abdel-Aziz A. M., Abou-Zeid L. A., Eldin K.,Tahir H. E, Ayyad R. R., El-SayedM. A. A. , El-Azab A. S. Synthesis, anti-inflammatory, analgesic, COX-1/2 inhibitory activities and molecular docking studies of substituted 2-mercapto-4(3*H*)-quinazolinones*European Journal of Medicinal Chemistry*121, 410-421, 2016.

Alagarsamy V., Raja Solomon V., Vanikavitha G., Paluchamy V., S. Amuthalakshmi S., Ravi Chandran M., Arnold Sujin A., Thangathirupathy A., Revathi R., Synthesis, Analgesic, Anti-inflammatory and Antibacterial Activities of Some Novel 2-Phenyl-3-substituted Quinazolin-4(3*H*)-Ones*Biol. Pharm. Bull.* 25, 1432-1435, 2002.

Amin K.M., Kamel M.M., Anwar M.M., Khedr M., Syam Y.M. Synthesis, biological evaluation and molecular docking of novel series of spiro [(2H,3H) quinazoline-2,10- cyclohexan]-4(1H)- one derivatives as anti-inflammatory and analgesic agents*European Journal of Medicinal Chemistry* 45, 2117–2131, 2010.

Manivannan E., Chaturvedi S. C. Analogue-based design, synthesis and molecular docking analysis of 2,3-diaryl quinazolinones as non-ulcerogenic anti-inflammatory agents *Bioorganic & Medicinal Chemistry* 19, 4520–4528, 2011.

Andrews S. P., Cox R. J. Small Molecule CXCR3 Antagonists*Journal of medicinal chemistry* 59, 2894−2917, 2016.

Abou-Seri S. M., Abouzid K., El Ella D.A. A. Molecular modeling study and synthesis of quinazolinone-arylpiperazine derivatives as a1-adrenoreceptor antagonists *European Journal of Medicinal Chemistry* 46, 647-658, 2011.

Chang F. R., Wu C. C., Hwang T. L., Patnam R., Kuo R. Y., Wang W. Y., Lan Y. H., Wu Y. C. Effect of active synthetic 2-substituted quinazolinones on anti-platelet aggregation and the inhibition of superoxide anion generation by neutrophils *Arch Pharm Res*26, 511-515, 2003.

Fry D.W., Kraker A.J., Michael A. M., Ambroso L. A., Nelson J. M., Leopold W. R., Connors R.W., Bridges A.J.A Specific Inhibitor of the Epidermal Growth Factor Receptor Tyrosine Kinase *Science* 265, 1093-1095, 1994.

Lewerenz A., Hentschel S., Vissiennon Z., Michael S., Nieber K.,A_3 receptors in cortical neurons: Pharmacological aspects and neuroprotection during hypoxia *Drug Development Research* 58,420-427, 2003.

Kashawa S. K., Kashawa V., Mishra P., Jain N.K.,Stables J.P Synthesis, anticonvulsant and CNS depressant activity of some new bioactive 1-(4-substituted-phenyl)-3-(4-oxo-2-phenyl/ethyl-4H-quinazolin-3-yl)-urea*European Journal of Medicinal Chemistry* 44, 4335–4343, 2009.

Reddy V., Reddy V., Allaka T., Anireddy J., Varala R. Synthesis and antibacterial activity studies of 6-methoxyquinazoline-triazole hybrid derivatives *Org. Commun*. 8, 98-108, 2015.

Jadhav R. P., Raundal H. N., Patil A. A., Bobade V. D. Synthesis and biological evaluation of a series of 1,4-disubstituted 1,2,3-triazole derivatives as possible antimicrobial agents*Journal of Saudi Chemical Society* 21, 152–159, 2017.

Shaikha M. H., Subhedara D. D., Khan F. A. K., Sangshetti J. N., Shingatea B. B. 1,2,3-Triazole incorporated coumarin derivatives as potential antifungal and antioxidant agents *Chinese Chemical Letters* 27, 295-301, (2016).

Kumar K., Ramakrishna G., Thakur R. K., Reddy V., Pandey J., Mahar R., shukla S. K., Tamrakar A. K., Tripathi R. P Synthesis of novel glycosyl-1,2,3-1*H*-triazolyl methyl quinazolin-4(3*H*)-ones and their effect on GLUT4 translocation *Tetrahedron*73, 187-203, 2017.

Zhao X., Lu B. W., Lu J. R., Xin C. W., Li J. F., Liu Y. Design, synthesis and antimicrobial activities of 1,2,3-triazole derivatives*Chinese Chemical Letters* 23, 933–935, 2012.

Selvam P., Girija K., Nagarajan G., Clercq D. E.,Synthesis, Antibacterial And AntiHIV Activities Of 3-(5-Amino-6-(2-3-Dichloro-Phenyl)-(1,2,4) Triazin-3-Yl)-6,8-Dibromo-2-Substituted-3H-Quinozolin-4-One*Indian J. Pharm. Sci*.67 484-487, 2005.

Wang D., Chen S., Wang J., Astruc D.,Chen B. Base-catalyzed hydrogen–deuterium exchange and dehalogenation reactions of 1,2,3-triazole derivatives *Tetrahedron* 72, 6375-6379, 2016.

Wenqiang T., Qing L., Huali W., Yan L., Jingjing Z., Fang D., Zhanyong G. Synthesis, characterization, and antibacterial property of novel starch derivatives with 1,2,3-triazole*Carbohydrate polymer* 142, 1-7, 2016.

Wang G., Peng Z., Wang J., Juan L., Xin L. Synthesis and biological evaluation of novel 2,4,5-triarylimidazole–1,2,3-triazole derivatives via click chemistry as α-glucosidase inhibitors*Bioorganic & Medicinal Chemistry Letters* 26, 5719–5723, 2016.

Suresh G.V.K, Rajendra Y. P., Mallikarjuna B. P., Chandrashekar S.M., Kistayya C., Synthesis of some novel 2-substituted-5-[isopropylthiazole] clubbed 1,2,4-triazole and 1,3,4-oxadiazoles as potential antimicrobial and antitubercular agents*Eur. J. Med. Chem*. 45, 2063–2074, 2010.

Ullaha H., Sainia K. S., Ajay A., Devender N., Bhattacharjee A., Dasa S., Dwivedi S. , Gupt M. P., Kousik H., Mitra B. K., Tripathi R. P.,Konwara R. Triazole analog 1-(1-benzyl-5-(4-chlorophenyl)-1H-1,2,3-triazol-4-yl)-2-(4-bromophenylamino)-1-(4-chlorophenyl)ethanol inducesreactive oxygen species and autophagy-dependent apoptosis in bothin vitro and in vivo breast cancer models*The International Journal of Biochemistry & Cell Biology* 65, 275–287, 2015.

El-Etrawy A. S., Abdel-Rahaman A. A. H. synthesis and antiviral evaluation of 1,3-dimethyl-6-(1h-1,2,3-triazol-1-yl)pyrimidine- 2,4(1h,3h)-dione derivatives *Chem. Heterocycl. Compd*. 46, 1105–1108, 2010.

Devender N., Gunjan S., Tripathi R., Tripathi R. P. Synthesis and antiplasmodial activity of novel indoleamide derivatives bearing sulfonamide and triazole pharmacophores*European Journal of Medicinal Chemistry* 131, 171-184, 2017.

Koohshari M., Dabiri M., Salehi P., Bahramnejad M.Multicomponent Synthesis of 1,2,3-Triazol-4-yl-methylthio-3- arylquinazolin-4(3H)-one Derivatives *Synthetic Communications* 42, 2415-2422, 2012.

Dave V. B., Thakor M. K. Design, synthesis and antimicrobial activity of some newer 3(H)-quinazoline-4-one derivative *J. Curr. Chem. Pharm. Sc*. 5, 99-104, 2015.

ChaudharyA. P., Bharti S. K., Kumar S., Kumar V., Kant P. Study of molecular structure, chemical reactivity and first hyperpolarizability of a newly synthesized N-(4-oxo-2-phenylquinazolin-3(4H)-yl)-1H-indole-2-carboxamide using spectral analysis *Journal of Molecular Structure*1148, 356-363, 2017.

Koysal Y., Tanak H. Crystal structure, spectroscopic investigations and density functional studies of 4-(4-methoxyphenethyl)-5-benzyl-2H-1,2,4-triazol-3(4H)-one monohydrate *Spectrochimica Acta Part A* 93, 106– 115, 2012.

Devender N., Gunjan S., Tripathi R., Tripathi R. P. Synthesis and antiplasmodial activity of novel indoleamide derivatives bearing sulfonamide and triazole pharmacophores*European Journal of Medicinal Chemistry* 131, 171-184, 2017.

Rawat P., Singh R.N. Assessment of conformational, spectral, antimicrobial activity, chemical reactivity and NLO application of Pyrrole-2,5-dicarboxaldehyde bis(oxaloyldihydrazone) *Spectrochimica Acta Part A: Molecular and Biomolecular Spectroscopy* 140, 344–355, 2015.

Rawat P., Singh R.N., Kumar A. Synthesis, molecular structure, photoluminescence, multiple interaction, chemical reactivity and first hyperpolarizability analysis of ethyl 2-cyano-3-{5-(4-methylbenzenesulfonyl)-hydrazonomethyl]-1*H*-pyrrol-2-yl}-acrylate: Experimental and quantum chemical approaches *Journal of Molecular Structure* 1061, 140–149, 2014.

Anitha E. G., Vedhagiri S. J., Parimala K. Conformational stability, vibrational spectra, NLO properties, NBO and thermodynamic analysis of 2-amino-5-bromo-6-methyl-4-pyrimidinol for dye sensitized solar cells by DFT methods *Spectrochimica Acta Part A: Molecular and Biomolecular Spectroscopy* 140, 544–562, 2015.

Kishor G. T., Nagaiyan S. Pyrrole-thiazole based push-pull chromophores: An experimental and theoretical approach to structural, spectroscopic and NLO properties of the novel styryl dyes *Journal of Photochemistry and Photobiology A: Chemistry*333, 1-17, 2017.

Natorajan S., Shanmugam G., Martin S.A. Growth and characterization of a new semi organic NLO material: L-tyrosine hydrochloride *Cryst. Res. Technal.* 43, 561-564, 2008.

Corresponding author: Padam Kant, Department of chemistry University of Lucknow, Lucknow Uttar Pradesh-226007, India
Email: Kant_padam@lkouniv.ac.in **anirudhraj0002@gmail.com**